



UNIVERSITY OF LEEDS

This is a repository copy of *Electron-phonon relaxation rates and optical gain in a quantum cascade laser in a magnetic field* .

White Rose Research Online URL for this paper:
<http://eprints.whiterose.ac.uk/1693/>

Article:

Radovanovic, J., Milanovic, V., Ikonc, Z. et al. (2 more authors) (2005) Electron-phonon relaxation rates and optical gain in a quantum cascade laser in a magnetic field. *Journal of Applied Physics*, 97 (10). 103109 -(5 pages). ISSN 1089-7550

<https://doi.org/10.1063/1.1904706>

Reuse

See Attached

Takedown

If you consider content in White Rose Research Online to be in breach of UK law, please notify us by emailing eprints@whiterose.ac.uk including the URL of the record and the reason for the withdrawal request.



eprints@whiterose.ac.uk
<https://eprints.whiterose.ac.uk/>

Electron-phonon relaxation rates and optical gain in a quantum cascade laser in a magnetic field

J. Radovanović

Institute of Physics, University of Belgrade, Pregrevica 118, 11080 Belgrade, Serbia and Montenegro

V. Milanović

Faculty of Electrical Engineering, Bulevar kralja Aleksandra 73, 11120 Belgrade, Serbia and Montenegro

Z. Ikonić,^{a)} D. Indjin, and P. Harrison

Institute of Microwaves and Photonics, School of Electronic and Electrical Engineering, University of Leeds, Woodhouse Lane, Leeds LS2 9JT, United Kingdom

(Received 26 January 2005; accepted 16 March 2005; published online 9 May 2005)

We present a model for calculating the optical gain in a midinfrared GaAs/AlGaAs quantum cascade laser in a magnetic field, based on solving the set of rate equations that describe the carrier density in each level, accounting for the optical- and acoustic-phonon scattering processes. The confinement caused by the magnetic field strongly modifies the lifetimes of electrons in the excited state and results in pronounced oscillations of the optical gain as a function of the field. Numerical results are presented for the structure designed to emit at $\lambda \sim 11.4 \mu\text{m}$, with the magnetic field varying in the range of 10–60 T. The effects of band nonparabolicity are also included. © 2005 American Institute of Physics. [DOI: 10.1063/1.1904706]

I. INTRODUCTION

The last decade has witnessed fast progress in the field of unipolar semiconductor quantum cascade lasers (QCLs), which are very promising candidates for practical sources of radiation, particularly in the midinfrared spectral range.^{1–7} Considerable output power, room-temperature operation, as well as the ability to get a range of lasing wavelengths using the same material system, opens up a number of potential applications for these devices, such as trace gas detection, pollution control, medical diagnostics, optical communications in high-transparency atmospheric windows, etc.⁴

QCL operation is based on intersubband optical transitions, between size-quantized states within the conduction band of multiple quantum well type structures. The excited state lifetimes in such systems are very short (~ 1 ps) because they are dominated by electron-longitudinal-optical (LO)-phonon scattering process. Consequently, the typical threshold currents in QCLs are much larger than is common for conventional interband lasers, with their much longer carrier lifetimes.⁷ However, it has been recently pointed out^{4–8} that considerable improvements in this respect (i.e., increased lifetimes of carriers in the excited state) might be achieved by effectively reducing the system dimensionality, e.g., by applying a strong magnetic field perpendicular to the layers. The magnetic field induces additional quantization of the in-plane electron motion, and the continuous two-dimensional (2D) subbands are split into a series of discrete Landau levels (LL). Their energies depend on the field, which, together with the fact that scattering rates between states are sensitive to their energy spacing, enables one to selectively enhance or inhibit different relaxation channels in a multilevel system by varying the magnetic-field strength.

In particular, the electron relaxation from the upper laser state into various states below it can be efficiently controlled in such a manner. This translates into a field-induced modulation of the population inversion and optical gain.

In this work we set a theoretical model for the calculation of electronic relaxation rates in the QCL active region in a strong magnetic field, due to optical- and acoustic-phonon-induced transitions between Landau levels, which enables one to find the electron distribution over the states of the system by solving the full set of rate equations describing the transitions between levels, and eventually determine the optical gain. Calculations are performed for a GaAs/Al_xGa_{1-x}As QCL structure designed to emit in the mid-IR range,^{5,6} for which the calculation of the upper laser state lifetime has previously been performed, and the experimental data are also available.^{5,6}

II. THEORETICAL CONSIDERATIONS

The active region of the QCL structure under consideration comprises three coupled quantum wells (QWs) biased by an external electric field K , as displayed in Fig. 1. In the absence of the magnetic field this system has three energy states, i.e., subbands ($n=1,2,3$), and the laser transition occurs between subbands $n=3$ and $n=2$. This active region is surrounded by suitable emitter/collector regions in the form of superlattices, designed as Bragg reflectors, which inject electrons into state $n=3$ on one side, and allow for rapid extraction of carriers from the lowest subband $n=1$, on the other side. The energy difference between E_2 and E_1 should match the LO-phonon energy in order to ensure fast depopulation of the lower state of the laser transition via resonant optical-phonon emission. These two mechanisms are responsible for achieving population inversion between subbands E_3 and E_2 .

^{a)}Electronic mail: eenzi@leeds.ac.uk

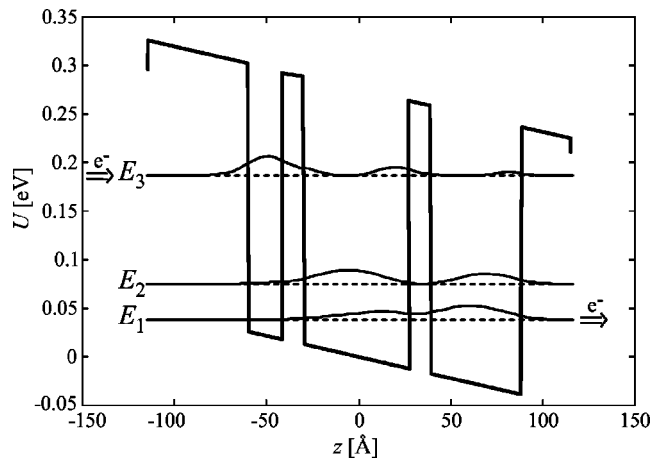


FIG. 1. The conduction-band diagram of the active region of GaAs/Al_{0.33}Ga_{0.67}As QCL described in Ref. 5, in an electric field of 44 kV/cm. The subband positions at zero magnetic field, together with the corresponding wave functions squared, are also displayed. The horizontal arrows indicate the flow of electrons, which are injected into the state $n=3$ and extracted from the state $n=1$.

In the direction parallel to the QW planes, the electronic states have free particlelike energy dispersion: $E = \hbar^2 k_{\parallel}^2 / 2m^*$, where m^* is the effective mass, and k_{\parallel} is the in-plane wave vector. The nonradiative lifetime for the state $|3, k_{\parallel}\rangle$ is limited by electron-LO-phonon scattering into the two lower subbands of the active region, and can therefore reach only picosecond values, which results in a considerable threshold current necessary to achieve the optical gain necessary for lasing. When the structure is subjected to a strong magnetic field B in the direction of the growth axis, continuous subbands $E_n(k_{\parallel})$ transform into series of individual (strictly discrete) states at energies $E_{n,l} \approx E_n + (l+1/2)\hbar\omega_c$, where $l=0, 1, 2, \dots$ is the Landau index and $\omega_c = eB/m^*$ is the cyclotron frequency. Variation of the magnetic field B influences the configuration of the discrete states, and hence the rates of electron-phonon relaxation processes. The values of B which give rise to resonant LO-phonon emission are found by solving the equation: $E_{3,0} - E_{n,l} = \hbar\omega_{LO}$, with $n=1, 2$, where $\hbar\omega_{LO}$ is the LO-phonon energy.

Optical transitions in this system are allowed only between states with the same value of the Landau index,⁹ i.e., $(i, l) \rightarrow (f, l)$. The fractional absorption (or, if it comes out to be negative, the gain) on transitions corresponding to the lasing energy, i.e., $(2, l) \rightarrow (3, l)$, reads:

$$A_{2,l \rightarrow 3,l} = \frac{2e^3 \pi B d_{2,3}^2 \delta(E_{3,l} - E_{2,l} - \hbar\omega) F_{2,l;3,l}}{\bar{n} \hbar \epsilon_0 \lambda}, \quad (1)$$

where ϵ_0 is the vacuum dielectric permittivity, \bar{n} is the material refractive index, c the velocity of light, $F_{i,f}$ is the difference of Fermi-Dirac functions for the initial and the final state, and $d_{if} = \langle \eta_i | z | \eta_f \rangle$ is the transition matrix element (with η_i and η_f denoting the z -dependent parts of the wavefunctions). Using the expression for the electron areal density in the state (n, l) , i.e., $N_{n,l} = eB / (\pi \hbar) F_{FD}(E_{n,l})$, and summing over all LLs, we get the total gain on all transitions between LLs belonging to subbands $n=3$ and $n=2$ of the QCL active region:

$$g_{3,2} = \frac{2e^2 \pi^2 d_{2,3}^2 \delta(E_{3,0} - E_{2,0} - \hbar\omega)}{\bar{n} \epsilon_0 \lambda} (N_{S3} - N_{S2}). \quad (2)$$

To determine the population inversion $N_{S3} - N_{S2}$, on which the gain depends, one has to find the electron distribution over all the states in the active region. This is obtained by solving the system of rate equations, which describe the change in level population as the difference between the rate at which the carriers arrive and the rate at which they leave. We assume that electrons arrive in the active region in Fig. 1 by a constant current with the areal density J , and are injected into only a limited number of LLs of the excited laser state, i.e., into levels $(3, 0); \dots; (3, l_{\max_3})$. The value l_{\max_3} is determined so that all the levels above $(3, l_{\max_3})$ may be considered as almost empty at a given temperature, if the carrier distribution among them was equilibriumlike. Neglecting the phonon absorption processes, which is justified at lower temperatures,¹⁰ the system of rate equations takes the form

$$\frac{\partial N_{3,l_{\max_3}}}{\partial t} = \frac{J_{3,l_{\max_3}}}{e} - N_{3,l_{\max_3}} \left[\sum_{p=0}^{l_{\max_3}-1} \frac{\bar{f}(E_{3,p})}{\tau_{3,l_{\max_3};3,p}} + \sum_{i=0}^{l_{\max_2}} \frac{\bar{f}(E_{2,i})}{\tau_{3,l_{\max_3};2,i}} + \sum_{j=0}^{l_{\max_1}} \frac{\bar{f}(E_{1,j})}{\tau_{3,l_{\max_3};1,j}} \right] = 0$$

:

$$\frac{\partial N_{3,k}}{\partial t} = \frac{J_{3,k}}{e} + \bar{f}(E_{3,k}) \left[\sum_{p=k+1}^{l_{\max_3}} \frac{N_{3,p}}{\tau_{3,p;3,k}} + \sum_{i=i_{\min(3,k)}}^{l_{\max_2}} \frac{N_{2,i}}{\tau_{2,i;3,k}} + \sum_{j=j_{\min(3,k)}}^{l_{\max_1}} \frac{N_{1,j}}{\tau_{1,j;3,k}} \right] - N_{3,k} \left[\sum_{p=0}^{k-1} \frac{\bar{f}(E_{3,p})}{\tau_{3,k;3,p}} + \sum_{i=0}^{l_{\min(3,k)}-1} \frac{\bar{f}(E_{2,i})}{\tau_{3,k;2,i}} + \sum_{j=0}^{j_{\min(3,k)}-1} \frac{\bar{f}(E_{1,j})}{\tau_{3,k;1,j}} \right] = 0$$

:

$$\frac{\partial N_{2,k}}{\partial t} = \bar{f}(E_{2,k}) \left[\sum_{p=p_{\min(2,k)}}^{l_{\max_3}} \frac{N_{3,p}}{\tau_{3,p;2,k}} + \sum_{i=k+1}^{l_{\max_2}} \frac{N_{2,i}}{\tau_{2,i;2,k}} + \sum_{j=j_{\min(2,k)}}^{l_{\max_1}} \frac{N_{1,j}}{\tau_{1,j;2,k}} \right] - N_{2,k} \left[\sum_{p=0}^{p_{\min(2,k)}-1} \frac{\bar{f}(E_{3,p})}{\tau_{2,k;3,p}} + \sum_{i=0}^{k-1} \frac{\bar{f}(E_{2,i})}{\tau_{2,k;2,i}} + \sum_{j=0}^{j_{\min(2,k)}-1} \frac{\bar{f}(E_{1,j})}{\tau_{2,k;1,j}} \right] = 0$$

:

$$\begin{aligned}
\frac{\partial N_{1,k}}{\partial t} &= \bar{f}(E_{1,k}) \left[\sum_{p=p_{\min(1,k)}}^{l_{\max_3}} \frac{N_{3,p}}{\tau_{3,p;1,k}} + \sum_{i=i_{\min(1,k)}}^{l_{\max_2}} \frac{N_{2,i}}{\tau_{2,i;1,k}} \right. \\
&\quad \left. + \sum_{j=k+1}^{l_{\max_1}} \frac{N_{1,j}}{\tau_{1,j;1,k}} \right] - N_{1,k} \left[\sum_{p=0}^{p_{\min(1,k)}-1} \frac{\bar{f}(E_{3,p})}{\tau_{1,k;3,p}} \right. \\
&\quad \left. + \sum_{i=0}^{i_{\min(1,k)}-1} \frac{\bar{f}(E_{2,i})}{\tau_{1,k;2,i}} + \sum_{j=0}^{k-1} \frac{\bar{f}(E_{1,j})}{\tau_{1,k;1,j}} \right] - \frac{J_{1,k}}{e} = 0 \\
&\vdots \\
\frac{\partial N_{1,1}}{\partial t} &= \bar{f}(E_{1,1}) \left[\sum_{p=p_{\min(1,1)}}^{l_{\max_3}} \frac{N_{3,1}}{\tau_{3,p;1,1}} + \sum_{i=i_{\min(1,1)}}^{l_{\max_2}} \frac{N_{2,i}}{\tau_{2,i;1,1}} \right. \\
&\quad \left. + \sum_{j=2}^{l_{\max_1}} \frac{N_{1,j}}{\tau_{1,j;1,1}} \right] - N_{1,1} \left[\sum_{p=0}^{p_{\min(1,1)}-1} \frac{\bar{f}(E_{3,p})}{\tau_{1,1;3,p}} \right. \\
&\quad \left. + \sum_{i=0}^{i_{\min(1,1)}-1} \frac{\bar{f}(E_{2,i})}{\tau_{1,1;2,i}} + \frac{\bar{f}(E_{1,0})}{\tau_{1,1;1,0}} \right] - \frac{J_{1,1}}{e} = 0, \quad (3)
\end{aligned}$$

where $\tau_{n_1,l_1;n_2,l_2}$ is the electron relaxation rate corresponding to nonradiative transitions from the state (n_1, l_1) to (n_2, l_2) , due to emission of both LO and acoustic phonons, and $\bar{f}(E_{n,l}) = 1 - (\pi\hbar)/(eB)N_{n,l}$. The injection and extraction currents are calculated as $J_{3,k} = J \exp(-E_{3,k}/k_B T) / \sum_{p=0}^{l_{\max_3}} \exp(-E_{3,p}/k_B T)$ and $J_{1,k} = J \exp(-E_{1,k}/k_B T) / \sum_{p=0}^{l_{\max_1}} \exp(-E_{1,p}/k_B T)$. Under steady-state conditions, the rate of change of subband populations in the active region equals zero. The radiative transition rates are several orders of magnitude smaller than the nonradiative transition rates and are therefore neglected in the system (3). The quantities l_{\max_1} and l_{\max_2} are the maximal values of Landau indices of levels originating from the two lower subbands, for which the following inequalities still hold true: $E_{3,l_{\max_3}} - E_{1,l_{\max_1}} > 0$ and $E_{3,l_{\max_3}} - E_{2,l_{\max_2}} > 0$. Upon solving the above system of $l_{\max_1} + l_{\max_2} + l_{\max_3} + 2$ nonlinear equations, supplemented with the particle conservation law: $\sum_{n,l} N_{n,l} = N_S$ (where N_S is the total electron sheet density, set by doping), we calculate the inversion and the optical gain in the QCL active region.

III. NUMERICAL RESULTS

The active region of a QCL based on the GaAs/Al_{0.33}Ga_{0.67}As heterostructure, described in Refs. 5 and 6, designed to emit radiation at 11.4 μm , is displayed in Fig. 1. The layer widths are 56, 19, 11, 58, 11, 49, and 28 \AA , going from the emitter towards the collector barrier, and the electric field is 44 kV/cm. The material parameters used in the calculation are $m^* = 0.0665m_0$ (m_0 is the free electron mass), $\bar{n} = 3.3$, and the conduction-band discontinuity between GaAs and AlAs is $\Delta E_c = 0.8355$ eV. In the absence of a magnetic field, the three subbands are at energies $E_1(k_{\parallel} = 0) = 76.5$ meV, $E_2(k_{\parallel} = 0) = 113.5$ meV, and $E_3(k_{\parallel} = 0) = 224.5$ meV, with the lasing transition energy of $E_3 - E_2 = 111$ meV in full agreement with the measured value.²

When this structure is subjected to a strong external magnetic field in the z direction, the 2D subbands $E_n(k_{\parallel} = 0) + \hbar^2 k_{\parallel}^2 / 2m^*$ split into series of discrete LLs, the energies of which (with band nonparabolicity included) are given by¹¹ $E_{n,l} = E_n(k_{\parallel} = 0) + (l + 1/2)\hbar eB / \bar{m}_{\parallel n}(E) - 1/8[(8l^2 + 8l + 5)\alpha'_1 + (l^2 + l + 1)\beta'_1](\hbar eB / m^*)^2$. The averaged in-plane electron effective mass is calculated here as $\bar{m}_{\parallel n}^{-1}(E) = \int \eta_n^2(z) m_{\parallel}^{-1}(z, E) dz$ (this provides the best agreement with the experimental results¹²), where $m_{\parallel}(z, E) = m^* \{1 + (2\alpha'_1 + \beta'_1)[E - U(z)]\}$, and $U(z)$ is the conduction-band profile from Fig. 1, while $\alpha'_1 = 0.642$ eV⁻¹ and $\beta'_1 = 0.679$ eV⁻¹ are the nonparabolicity parameters. The LO-phonon emission rate on the transitions between the initial state $E_i = E_{n_i, l_i}$ and the final state $E_f = E_{n_f, l_f}$ is given by¹³

$$\begin{aligned}
W_{\text{LO}}(E_i, E_f) &= \frac{e^2 \omega_{\text{LO}}}{\pi \epsilon_p} \delta[E_{n_i, l_i} - E_{n_f, l_f} - \hbar \omega_{\text{LO}}] \\
&\quad \times \int_0^{\infty} P^2(q_z) dq_z \int_0^{\infty} q_{\parallel} \frac{|F(q_{\parallel}, l_i, l_f)|^2}{q_z^2 + q_{\parallel}^2} \\
&\quad \times dq_{\parallel} [n_0(\hbar \omega_{\text{LO}}) + 1], \quad (4)
\end{aligned}$$

where $P = \int_0^d \eta_i^* \sin(q_z z) \eta_j dz$. Here d denotes the length of the confining region in the z direction, and q_z is the z projection of the phonon wave vector $q = (q_z, q_{\parallel})$. The quantity $|F(q_{\parallel}, l_i, l_f)|$ is the lateral overlap integral, the analytic expression for which, in the case $l_i \leq l_f$, reads

$$|F(q_{\parallel}, l_i, l_f)|^2 = \exp\left(-\frac{q_{\parallel}^2}{2\beta}\right) \frac{l_i!}{l_f!} \left(\frac{q_{\parallel}^2}{2\beta}\right)^{l_f - l_i} [L_{l_i}^{l_f - l_i}(q_{\parallel}^2 / 2\beta)]^2, \quad (5)$$

where $\beta^{-1} = (eB/\hbar)^{-1/2}$ is the magnetic length, and $L_n^k(x)$ denotes the associated Laguerre polynomial. For the case $l_i > l_f$ one simply swaps l_i and l_f in Eq. (5). The constant ϵ_p in Eq. (4) is calculated as $\epsilon_p^{-1} = \epsilon_{\infty}^{-1} - \epsilon_s^{-1}$, where ϵ_{∞} and ϵ_s are the high frequency and static permittivity, respectively, while $n(\hbar \omega_{\text{LO}}) = [\exp(\hbar \omega_{\text{LO}} / k_B T) - 1]^{-1}$ is the equilibrium population of optical phonons. The Dirac function in Eq. (4) expresses the energy conservation in transitions between discrete states (n_i, l_i) and (n_f, l_f) , but in a practical calculation one has to consider all states as broadened, with a Gaussian-like energy distribution.⁶ The widths of these Gaussians are taken to depend on B in the following manner: (1) $\sigma(B) = \sigma_0 \sqrt{0.5B}$, with $\sigma_0 = 1$ meV/ $T^{1/2}$, for transitions between states belonging to the same subband¹⁴ ($n_i = n_f$); (2) $\sigma = \sqrt{\pi/2}\Gamma$ if $n_i \neq n_f$, but matching Landau indices ($l_i = l_f$); and finally (3) $\sigma_{\text{eff}} = [0.5\sigma_0^2 B + (\pi/2)\Gamma^2]^{1/2}$ [meV], if $n_i \neq n_f$, $l_i \neq l_f$. Similarly, the Dirac function in the expression for optical gain (2) is replaced by a Lorentzian, with the linewidth parameter Γ . In addition to the LO phonons, we have also included the acoustic-phonon emission in the model, and the corresponding relaxation rate is given by^{10,13}

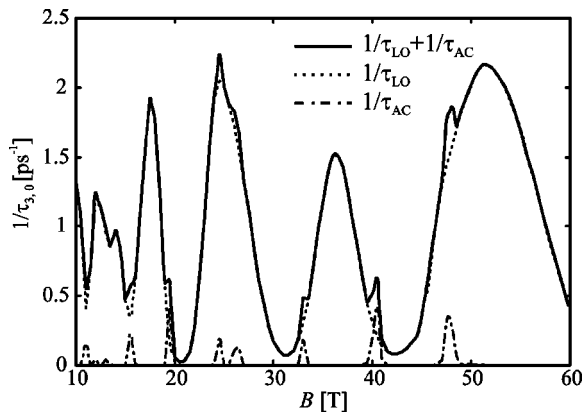


FIG. 2. The total electron relaxation rate due to emission of optical and acoustic phonons as a function of magnetic field, for transitions from the state (3,0) into LLs belonging to the two lower subbands.

$$W_{AC}(E_i, E_f) = \frac{\alpha_{AC} (E_i - E_f)^2}{\pi \hbar} \frac{1}{\hbar v_L} \frac{1}{-1 + \exp\left(-\frac{(E_i - E_f)}{k_B T}\right)} \times \int_0^{q_{z_{\max}}} P^2(q_z) dq_z |F(q_{l_0}, l_i, l_f)|^2 dq_z, \quad (6)$$

where $\alpha_{AC} = \Xi^2 / c_L$, Ξ is the deformation potential, c_L is the elastic constant associated with acoustic vibrations, $q_{z_{\max}} = [(E_i - E_f) / \hbar v_L]$, $q_{l_0} = [q_{z_{\max}}^2 - q_z^2]^{1/2}$, and v_L is the longitudinal-phonon velocity. Numerical parameters used in the calculations are $\epsilon_{\infty} = 10.67$, $\epsilon_s = 12.51$, $\Xi = 6.7$ eV, $c_L = 1.2 \times 10^{11}$ N/m², $v_L = 4.7 \times 10^3$ m/s, $\Gamma = 2.125$ meV, and $T = 77$ K.

The total relaxation rate for transitions from the ground LL of the third subband (into which the majority of carriers are injected) into the two sets of LLs of the two lower subbands is shown in Fig. 2, for the magnetic fields in the range of 10–60 T. Oscillations of the relaxation rate with B are very pronounced, and very prominent peaks are found at values of the magnetic field which satisfy the resonance conditions for LO-phonon emission. Conversely, when the ar-

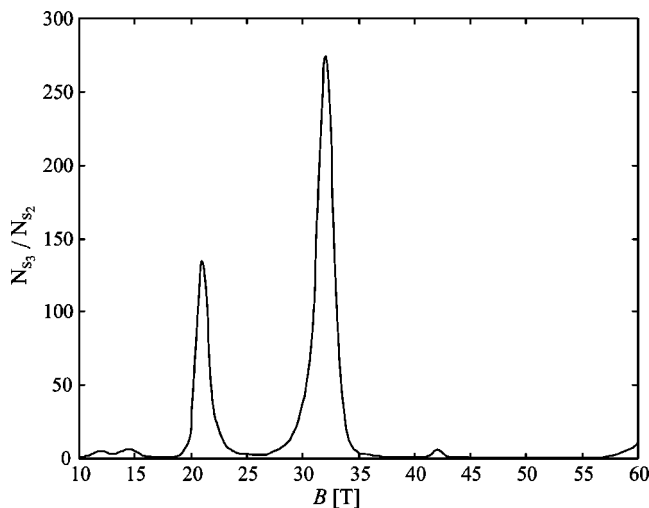


FIG. 3. The ratio of the total electron areal densities, in all LLs of the third and second subband, as a function of the magnetic field.

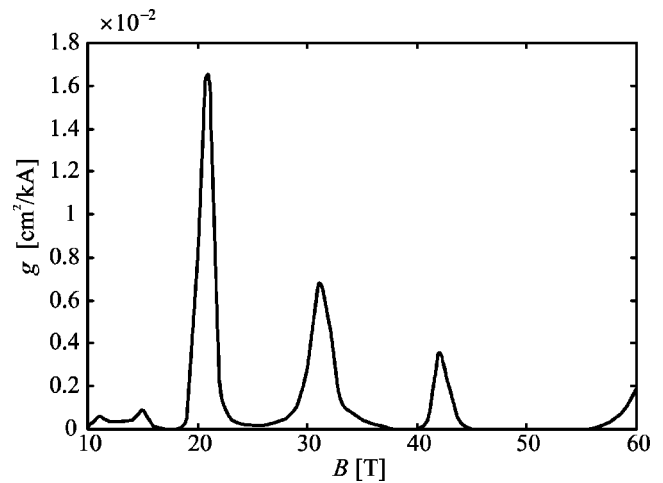


FIG. 4. The optical gain (per unit of injection current) as a function of the applied magnetic field, at $T = 77$ K.

range of LLs is such that there is no level situated at $\approx \hbar \omega_{LO}$ below the state (3,0), this type of scattering is inhibited, and therefore the lifetime of the upper laser state is increased. Results given in Fig. 2 compare very well with those in Ref. 5, except that the peaks here are broader, probably because of differences in modeling the state widths σ . One can also see from Fig. 2 that the relaxation rate via acoustic phonons is almost an order of magnitude smaller than via LO phonons.

Assuming a constant current injection, the modulation of lifetimes of all the states in the system results in either a suppression or an enhancement of population inversion between states (3,0) and (2,0), Fig. 3, and therefore also in modulation of the optical gain $g \approx g_{3,2} / J$, Fig. 4. The most prominent maximum of the gain is achieved at the magnetic field of $B = 20.5$ T, and the positions of relevant states in this case are displayed in Fig. 5. Electron relaxation from state (3,0) is clearly suppressed, because there is no lower state with energy around $E_{3,0} - \hbar \omega_{LO}$, and the lifetime for this state is as large as $\tau_{3,0} = 48.5$ ps in this case. Quite a different situation occurs at a field of $B = 24.5$ T. The configuration of

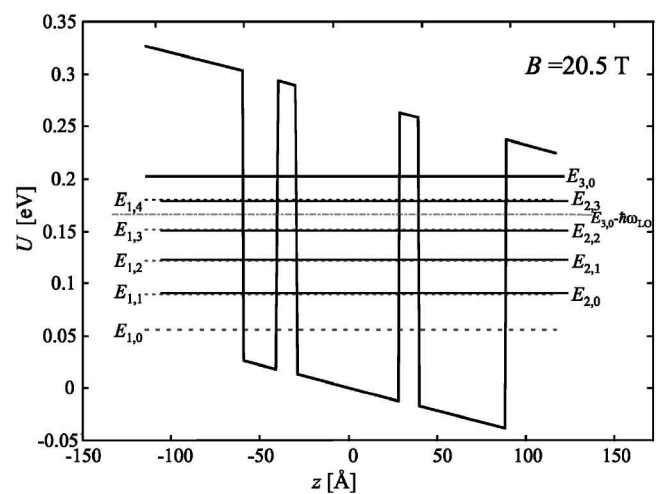


FIG. 5. Positions of relevant discrete states in the structure for the magnetic field of $B = 20.5$ T.

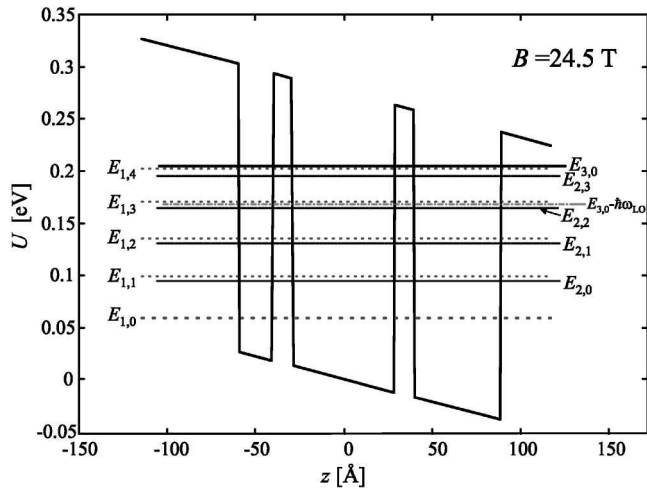


FIG. 6. Positions of relevant discrete states in the structure for the magnetic field of $B=24.5$ T.

relevant electronic states, shown in Fig. 6, leads to maximally enhanced relaxation rate from the (3,0) state, because there are now two states—(2,2) and (1,3)—which are $\approx \hbar\omega_{LO}$ below the upper laser state, and its lifetime is drastically reduced ($\tau_{3,0}=0.45$ ps). The result is a diminished inversion, and a minimum of optical gain, Fig. 4. Comparison of Figs. 3 and 4 with the positions of the light intensity minima and maxima given in Ref. 6 again shows a good agreement. Finally, we should note that throughout the above considerations we have assumed that the energy relaxation in the injector/collector is not sensitive to the magnetic field. This is likely to be a reasonable approximation since these regions consist of a multitude of extended states with small energy separation.⁷

IV. CONCLUSION

We have set up a rate equations based model and analyzed the optical gain in the active region of a quantum cascade laser in a magnetic field perpendicular to the structure layers. The field induces in-plane quantization of electron states and, with the energies of Landau levels depending on the field strength, enables tuning of relative positions of Landau levels so to strongly modulate the electron relaxation rates by positioning some states on or off resonance for LO-

phonon emission. These nonradiative relaxation processes may limit the output power of the QCL or even prevent lasing action at some values of the magnetic field, or, on the other hand, enhance the optical gain for other values of the field. The model presented for the calculation of electron-phonon scattering rates between Landau levels accounts for both the LO and acoustic-phonon emissions. It was applied to a GaAs/AlGaAs-based QCL structure, designed to emit radiation at $11.4 \mu\text{m}$, for which the potential of the magnetic field as a tool for controlling the phonon-assisted transfer has been studied experimentally, and for which the calculation of the upper state lifetime has been performed. The results of the more elaborate, rate equations model presented here show good agreement with the previous experimental and theoretical works, indicating the potential of extending this model towards including magnetic-field effects in the injector/collector regions (where electron-electron scattering is very important, and should be included) in order to get a more complete picture of processes in the whole structure.

ACKNOWLEDGMENTS

This work was funded by the Ministry of Science (Rep. Serbia), The Royal Society (UK), and EPSRC (UK). The authors would also like to thank O. Drachenko for his suggestions on modeling the band nonparabolicity.

- ¹C. Sirtori, P. Kruck, S. Barbieri, P. Collot, J. Nagle, M. Beck, J. Faist, and U. Oesterle, *Appl. Phys. Lett.* **73**, 3486 (1998).
- ²P. Kruck, H. Page, C. Sirtori, S. Barbieri, M. Stellmacher, and J. Nagle, *Appl. Phys. Lett.* **76**, 3340 (2000).
- ³H. Page, C. Becker, A. Robertson, G. Glastre, V. Ortiz, and C. Sirtori, *Appl. Phys. Lett.* **78**, 3529 (2001).
- ⁴T. Chakraborty and V. Apalkov, *Adv. Phys.* **52**, 455 (2003).
- ⁵D. Smirnov, O. Drachenko, J. Leotin, H. Page, C. Becker, C. Sirtori, V. Apalkov, and T. Chakraborty, *Phys. Rev. B* **66**, 125317 (2002).
- ⁶D. Smirnov, C. Becker, O. Drachenko, V. V. Rylkov, H. Page, J. Leotin, and C. Sirtori, *Phys. Rev. B* **66**, 121305 (2002).
- ⁷C. Becker, C. Sirtori, O. Drachenko, V. Rylkov, D. Smirnov, and J. Leotin, *Appl. Phys. Lett.* **81**, 2941 (2002).
- ⁸J. Alton *et al.*, *Phys. Rev. B* **68**, 081303 (2003).
- ⁹S. Živanović, V. Milanović, and Z. Ikončić, *Phys. Rev. B* **52**, 8305 (1995).
- ¹⁰G. Sun and J. Khurgin, *IEEE J. Quantum Electron.* **29**, 1104 (1993).
- ¹¹U. Ekenberg, *Phys. Rev. B* **40**, 7714 (1989).
- ¹²O. Drachenko (private communication).
- ¹³P. J. Turley, S. W. Teitsworth, and B. K. Bose, *J. Appl. Phys.* **72**, 2356 (1992).
- ¹⁴T. Ando, A. B. Fowler, and F. Stern, *Rev. Mod. Phys.* **54**, 437 (1982).